Positron studies of precipitation phenomena in Al-Li and in Al-LI-X (X=Cu, Mg or Sc) alloys

1992 J. Phys.: Condens. Matter 4 6317

(http://iopscience.iop.org/0953-8984/4/29/015)

J. Phys.: Condens. Matter 4 (1992) 6317–6328. Printed in the UK

Positron studies of precipitation phenomena in Al–Li and in Al–Li–X (X=Cu, Mg or Sc) alloys*

G Dlubek†‡, S Krause‡, H Krause‡, A L Beresina§, V S Mikhalenkov§ and K V Chuistov§

† (present address) Block 542/1, Edvard-Grieg-Weg 8, D(O)-4090 Halle, Federal Republic of Germany

‡ FB Physik, Pädagogische Hochschule, PF 763, D(O)-4002 Halle, Federal Republic of Germany

§ Institute of Metal Physics, Academy of Science of Ukraine, 252680 Kiev 142, Vernadsky Street 36, Ukraine

Received 16 March 1992

Abstract. Positron lifetime measurements were used for studying decomposition during post-quench *in situ* annealing of binary Al–7.35 at.% Li and ternary Al–7.3 at.% Li–X (X= 1.1 at.% Cu, 5.2 at.% Mg or 0.18 at.% Sc) alloys. A typical lifetime of 185 ± 5 ps observed in Al–Li is attributed to coherent $\delta'(Al_3Li)$ particles. In ternary alloys positrons show a strong response to the formation of semicoherent and incoherent phases such as $T_1(Al_2LiCu)$ and Al_2LiMg. Positron trapping in Al–Li–Sc is attributed to composite $\delta'(Al_3Li)/Al_3Sc$ particles associated with vacancies. Quenched-in vacancies were detected in Al–Li–Sc and Al–Li–Mg but not in Al–Li–Cu and Al–Li.

1. Introduction

The addition of lithium to aluminium produces an alloy of low density and high elastic modulus, and therefore the use of such alloys for various aircraft components results in substantial weight savings. That is the background of the increasing interest in the development of aluminium–lithium based alloys (see for example reviews [1–4] and references therein). In post-quench aged binary Al–Li alloys containing between 5.2 at.% and 14 at.% lithium, the $\delta'(Al_3Li)$ phase nucleates homogeneously and grows as a fully coherent precipitate with an $L1_2$ structure. This is the major strengthening phase, and when dislocations shear precipitate particles with an ordered structure like this, antiphase boundaries are generated, which gives rise to paired dislocation movement. The planar slip associated with these 'superdislocations' may lead to low ductility. Thus strengthening additions of Cu and/or Mg are made, leading to the nucleation of phases that aid slip homogenization. These phases may include all phases occurring in the binary as well as ternary alloys such as Al_2CuLi, Al_2MgLi and Al_2CuMg. Commercial alloys contain additionally small amounts of zirconium, which retards the recrystallization and leads to a grain refinement. It has, however, also an effect on the precipitate structure. Zirconium may be substituted by scandium, which has a similar effect on the microstructure [5, 6].

* Dedicated to Professor P Haasen on the occasion of his 65th birthday.

0953-8984/92/296317+12$04.50

The aim of the present paper is to study the precipitation processes going on during post-quench annealing of Al–Li based alloys by utilizing the positron lifetime technique. The investigations are focused on laboratory alloys of Al–Li, Al–Li–Cu, Al–Li–Mg and Al–Li–Sc. Extended experiments performed in the past on conventional Al alloys containing Zn, Mg, Ag, Cu or Si have indicated the potential of the positron annihilation technique in studying precipitation phenomena on an atomic or submicroscopic scale [7–10]. In the literature only a few papers are related to positron studies of Al–Li alloys [11, 12]. The behaviour of positrons in lithium-containing alloys may differ from that in other alloys owing to the high affinity of positrons to lithium atoms [13, 14], which may complicate the interpretation of positron experiments.

The paper is organized as follows. In the next section the interaction of positrons in decomposed alloys and the information given by positron lifetime measurements are briefly reviewed. Subsequently experimental details are given. The fourth section includes the discussion of results for binary and ternary Al–Li alloys followed by conclusions in section 5.

2. Interaction of positrons in decomposed alloys

In metals positrons may be trapped by open-volume lattice defects such as vacancies, vacancy–impurity complexes, vacancy clusters, voids, bubbles and dislocations [15, 16]. Mainly because of the missing positive ions, positrons feel an attractive potential at these defects, which leads to positron bound states of some eV binding energy [17]. Positrons localized at defects such as vacancies experience a lower electron density than delocalized positrons. Since the positron lifetime is inversely proportional to the overlap of positron and electron densities, this results in an increase of the trapped positron lifetime τ_t by a factor of about 1.5 compared with the lifetime of delocalized positrons (bulk lifetime τ_b). As discussed in earlier reviews [8, 9], semicoherent and incoherent particles formed in decomposed alloys may also act as positron traps. Positrons may become localized at the incoherent particle–matrix interface or at misfit dislocations. The trapped positron lifetime corresponds closely to that of a dislocation or of a vacancy.

Coherent particles such as Guinier–Preston (GP) zones may also trap positrons if they are associated with a potential that is attractive to positrons [8, 9]. The potential experienced by a positron at a coherent precipitate of B atoms in a matrix of A atoms may be estimated from the difference of the positron affinities $A_B - A_A$, that is the relative positron affinity. The positron affinity A is defined as the sum of the internal electron and positron chemical potentials [14]. In table 1 the relative positron affinity of different elements in relation to aluminium is given together with bulk and defect positron lifetimes. $A_B - A_A$ may have a negative or positive sign, resulting in an attraction or repulsion of positrons. As can be seen from table 1, the elements Li, Cu, Mg and Sc attract positrons in an Al matrix. The same is true for coherent particles of the Al_3Li phase, the affinity of which may be estimated in a good approximation [14] from the linear average of A_{Al} and A_{Li}, $A(Al_3Li) - A_{Al} = -0.74$ eV.

It is well known that single impurity atoms do not have a positron bound state but small clusters enriched in B atoms may localize positrons. This picture is confirmed by sophisticated quantum-mechanical calculations [10]; experimental evidence was given for GP zones in Al–Zn alloys [10, 18, 19] and in Al–Ag alloys [20]. However, lithium is a solid element with the strongest affinity to positrons. This may complicate the

Table 1. Bulk and trapped positron lifetime values and relative positron affinities $A_X - A_{Al}$ of various metals; $A_{Al} = -4.41$ eV.

Material	Positron lifetime (ps)			Relative positron affinity, $A_X - A_{Al}$ (eV) [14]
	Bulk	Vacancy	Dislocation	
Al	165	245 [28]	235 [44]	0
Li	293 [45]	312 [24][a]		−2.95
Cu	110 [46]	180 [46]	150 [47]	−0.40
Mg	225 [48]	253 [48]		−1.77
Sc	230 [49]			−0.69

[a] Theoretical estimate.

situation. As calculated by Puska and Manninen [21], light impurities may localize positrons. The positron binding energy of an empty vacancy and a vacancy occupied by one atom of hydrogen, helium or lithium is decreased as 2.90, 2.39, 1.67 and 0.42 eV, respectively. More recently, however, it was found by improved calculations that not a single Li atom but a cluster of four Li atoms may be able to localize a positron [22].

The lifetime of positrons annihilating from internal regions of coherent particles may be estimated in a first approximation from the average of the annihilation rates λ_i weighted with the atomic concentration of the elements forming the particles (see discussion in [23]). The annihilation rate λ is the inverse of the mean positron lifetime τ, $\lambda = 1/\tau$. We have estimated a positron lifetime of ~ 180 ps to be typical of the Al_3Li phase. For the lithium reference we have used a value of 260 ps. This value was estimated from the empirical rule given by Seeger and Banhart [24] taking into account the compression of a lithium atom in the aluminium matrix. The atomic volume in FCC aluminium amounts to 0.76 compared with BCC lithium, the positron lifetime of which amounts to 293 ps.

The changes of the annihilation characteristics as a function of the number of positron traps are described by the so-called trapping model [15, 16]. When there is only one type of positron trap, the positron lifetime spectrum is a sum of two exponential functions, the time constants $\tau_{1,2}$ and intensities $I_{1,2}$ of which are given by

$$\tau_1 = 1/(1/\tau_b + \kappa) \qquad \tau_2 = \tau_t \tag{1}$$

$$I_1 = 1 - I_2 \qquad I_2 = \kappa/(1/\tau_1 - 1/\tau_2). \tag{2}$$

Here τ_b and τ_t denote bulk and trapped positron lifetimes, and κ is the positron trapping rate. In the case of extended positron traps such as voids, GP zones or precipitated particles, the positron trapping rate is diffusion-limited and follows the relation $\kappa = 4\pi D_+ r N$, where r and N are the radius and the number per cubic metre of positron traps, assumed to be of spherical shape; $D_+ = 10^{-4}$ m^2 s^{-1} is the positron diffusion constant for Al [25].

3. Experimental details

The alloys under investigation were prepared in the Institute of Metal Physics, Kiev, from components of 99.99 wt% purity. The composition of the alloys is shown in

table 2. The composition of the Al–Li–Cu alloy corresponds to that of a commercial 2090 alloy, while the composition of Al–Li–Mg corresponds to the commercial 1420 alloy developed in the USSR [26]. Commercial materials contain about 0.1 wt% Zr and impurities (Si, Fe), which are absent in our laboratory alloys. For reference purposes a well annealed, pure (99.999 wt%) aluminium sample was also investigated.

Table 2. Composition (wt%/at.%) of alloys under investigation.

Alloy	Li	Cu	Mg	Sc
Al–Li	2.0/7.35	—	—	—
Al–Li–Cu	2.0/7.5	2.8/1.1	—	—
Al–Li–Mg	2.0/7.3	—	5.0/5.2	—
Al–Li–Sc	2.0/7.35	—	—	0.3/0.18

After homogenization annealing of the alloys for 10 h at 500 °C, sheets of 2 mm thickness were cut from a central part of the ingot. The sheets were solution-annealed at 520 °C for 0.5 h in argon gas and quenched into water at room temperature. Subsequently surface layers of 0.5 mm were removed by electropolishing using one-third nitric acid and two-thirds methanol. During polishing the samples warmed up to about 50 °C. The surface preparation is necessary because of the severe loss of lithium in surface regions during solution annealing. The lithium-depleted layer was examined by microhardness measurements. It may extend to some tenths of a millimetre in depth depending on the temperature and time of solution treatment. Since the positron implantation profile is an exponentially decreasing function with a typical (99%) penetration range in aluminium of 0.5 mm, the removal of the depleted surface layer is very important for studying Al–Li alloys by positrons.

Positron lifetime measurements were carried out during *in situ* annealing of quenched samples using a conventional fast–slow coincidence system [27]. Two identical samples were sandwiched with a 4×10^5 Bq positron source, which was made by evaporating carrier-free ^{22}NaCl solution on an aluminium foil of 10 μm thickness. The time resolution of the system was 230 ps (FWHM). Each spectrum was measured for 165 min to obtain 10^6 pulses. The measured lifetime spectra were analysed after source background subtraction as the sum of exponential lifetime components. One or in some cases two components enable a satisfactory fit. The results are presented in figures 1 to 5, which show the analysed lifetimes τ_1 and τ_2, the relative intensity I_2 and the average positron lifetime $\bar{\tau} = I_1\tau_1 + I_2\tau_2$.

4. Results and discussion

4.1. Al–Li alloy

The behaviour of the average positron lifetime $\bar{\tau}$ in the binary Al–Li and the ternary Al–Li–(Cu or Mg) alloys is shown in figure 1 as a function of the *in situ* annealing temperature together with the results of pure aluminium. In well annealed aluminium positrons annihilate near room temperature from a single, delocalized state. The experimental lifetime of 165 ps corresponds to the bulk lifetime of positrons, τ_b^{Al}. The positron lifetime increases almost linearly with temperature due to lattice expansion and phonon effects. Above 230 °C, $\bar{\tau}$ increases more strongly and a second lifetime

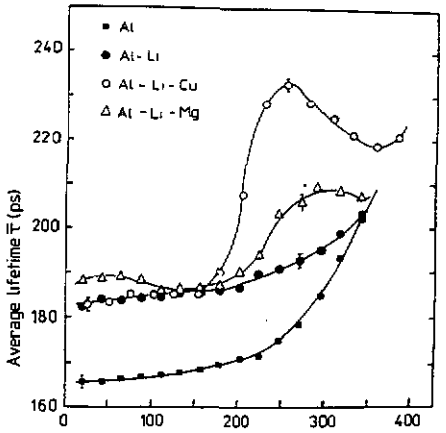

Figure 1. Behaviour of the average positron lifetime $\bar{\tau}$ during post-quench *in situ* annealing (165 min per experimental point) of Al–7.35 at.% Li, Al–7.5 at.% Li–1.1 at.% Cu and Al–7.3 at.% Li–5.2 at.% Mg alloys. For reference purposes well annealed Al (99.999% purity) was also investigated.

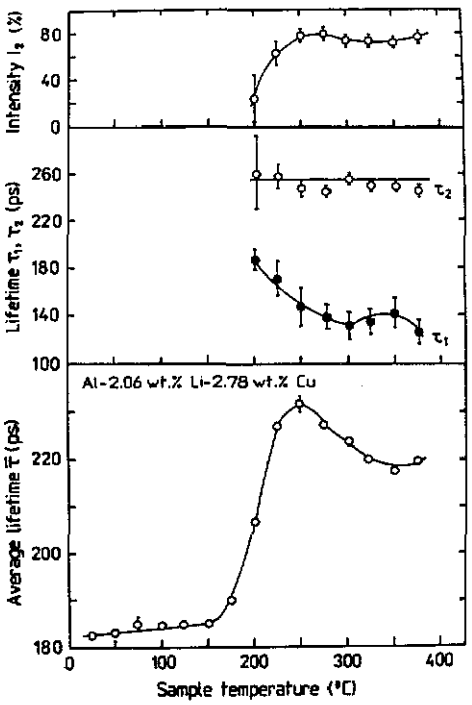

Figure 2. Parameters of the two-component decomposition of positron lifetime spectra as a function of the *in situ* annealing temperature in Al–7.5 at.% Li–1.1 at.% Cu.

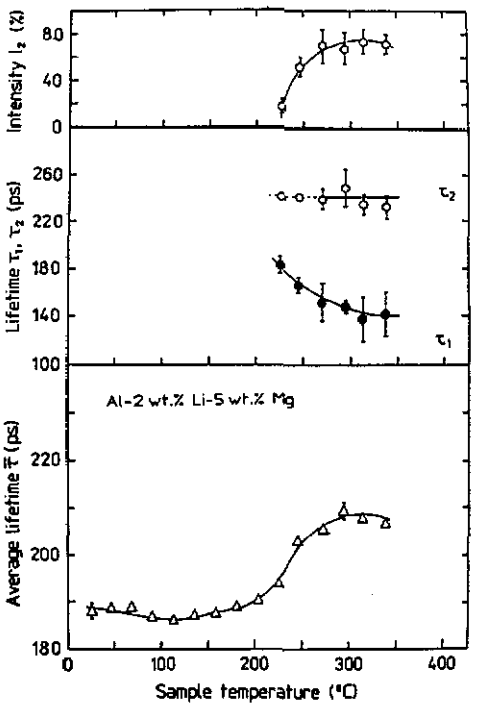

Figure 3. Same as figure 2 but Al–7.3 at.% Li–5.2 at.% Mg.

component with a lifetime of $\tau_2 = 240 \pm 5$ ps appears. This lifetime component is attributed to positron trapping by thermal vacancies, $\tau_2 = \tau_v^{Al}$ [28]. The increase in the average positron lifetime $\bar{\tau}$ with increasing temperature is due to the increase in the positron trapping rate κ, which is proportional to the thermal vacancy concentration.

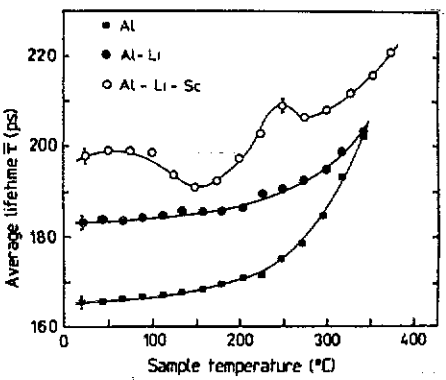

Figure 4. Same as figure 1 but Al–7.35 at.% Li–0.18 at.% Sc.

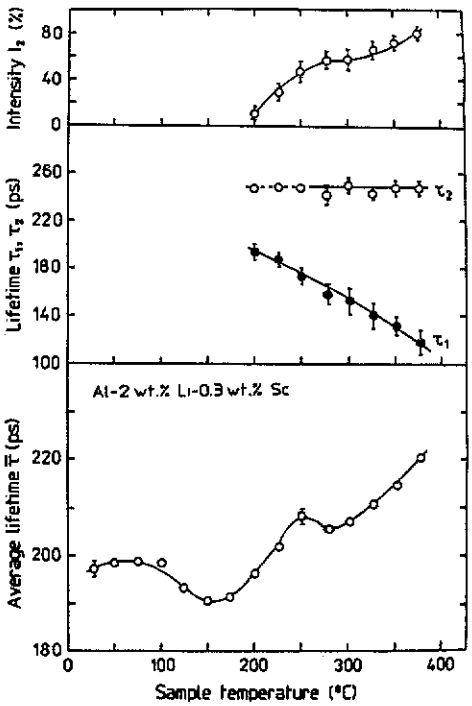

Figure 5. Same as figure 2 but Al–7.35 at.% Li–0.18 at.% Sc.

In Al–7.35 at.% Li the positron lifetime spectra are single exponential functions in the temperature range between room temperature and 250 °C. Near room temperature the lifetime in various Al–7.35 at.% Li samples ranges from 183 to 187 ps. Some fluctuations in $\bar{\tau}$ in addition to the statistical error of ± 2 ps may appear due to difficulties in reproducible surface preparation of Al–Li alloy samples. A lifetime component that might be attributed to quenched-in vacancies was never observed in binary Al–Li alloys. A high Li-to-vacancy binding energy of 0.25 eV was previously reported from resistivity measurements [29]. However, the Li atom–vacancy complexes may become mobile and disappear at sinks below room temperature.

The generally accepted decomposition of a supersaturated Al–Li solid solution (sss) has the form (see [1] and references therein)

$$\text{sss} \rightarrow \text{precursor phase to } \delta' \rightarrow \delta'(\text{Al}_3\text{Li}) \rightarrow \delta(\text{AlLi}).$$

There is an increasing discussion on the existence and nature of a precursor phase to δ'. Recent results of several authors agree with the picture that the Al–Li solid solution decomposes on quenching into a modulated order/disorder structure [30, 31]. In the temperature range fromn 100 to 200 °C the $\delta'(\text{Al}_3\text{Li})$ phase precipitates homogeneously in the form of spherical particles while the lithium content of the matrix lowers to about 5 at.%. As δ' has an ordered $L1_2$ superlattice structure, it is fully coherent with the matrix with a lattice misfit of $\delta a/a \leqslant -0.1\%$ [1] and may grow to 300 nm in diameter without loss of coherence; δ' loses Li stoichiometry as the

temperature increases. From field ion microscopy (FIM)/atom probe investigations Al-Kassab *et al* [32] have estimated a lithium content of 20.5 at.% in δ' particles formed at 190 °C. Above 230 °C, δ' dissolves in Al–7.2 at.% Li and incoherent particles of the δ(AlLi) phase (cubic B 32 structure) are nucleated heterogeneously at grain boundaries.

In the temperature range between 150 and 200 °C the Al–Li alloy is in a well decomposed state, which consists of spherical $\delta'(Al_3Li)$ particles homogeneously distributed in the α' (5 at.% Li) matrix (see figure 6(*a*)). In this temperature range we observed a typical positron lifetime of 185 ± 5 ps not only in Al–7.35 at.% Li but also in Al–10.8 at.% Li. This lifetime we attribute to positrons annihilating from internal regions of $\delta'(Al_3Li)$ particles. The high positron affinity of lithium promotes trapping of positrons by the coherent δ' particles. The experimental lifetime of 185 ± 5 ps is only slightly larger than our rough estimate of ~ 180 ps from section 2. Since any vacancy-type lifetime component does not appear below 250 °C, we may definitely conclude that the δ' phase is not associated with structural or interface vacancies.

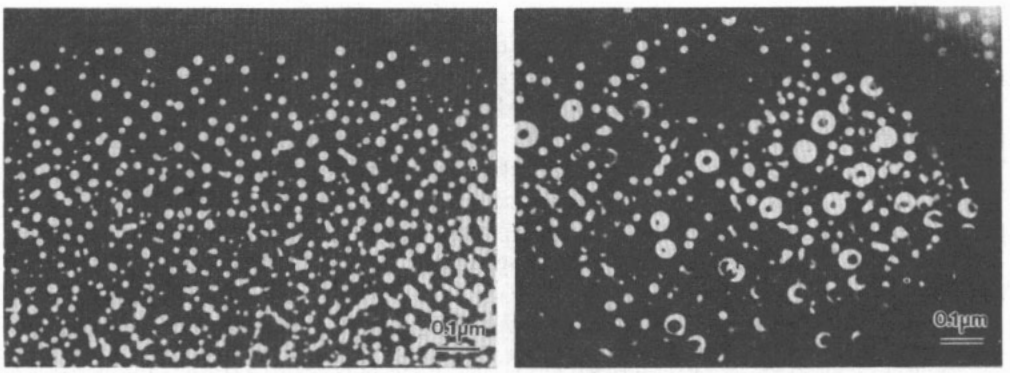

Figure 6. Transmission electron microscope centred dark-field images of a (1 1 0) δ' superlattice reflection. The samples were post-quench aged at 170 °C for 135 h. (*a*) Al–7.35 at.% Li; (*b*) Al–7.35 at.% Li–0.18 at.% Sc.

The weak change of the positron lifetime below 100 °C seems surprising. A value of 170 ps is expected for the disordered Al–7.35 at.% Li alloy. The experimental lifetimes, however, exceed 180 ps. Possibly, the preferential interaction of positrons with the precursor phase to δ' results in a positron lifetime like that of δ'. The $L1_2$ ordered regions formed quickly after quenching are expected to be enriched in lithium although they may not yet have the stoichiometric composition of δ' [1, 31].

Above 280 °C a second lifetime component with $\tau_2 = 245 \pm 20$ ps appears, which is the consequence of positron trapping by thermal vacancies. An additional contribution of particles of the incoherent δ phase to the long-life component is possible. But the effect of δ on positron trapping is expected to be small. Owing to the heterogeneous nucleation of δ at grain boundaries, its distribution is very inhomogeneous, which reduces the positron trapping.

4.2. Al–Li–Cu and Al–Li–Mg alloys

The behaviour of the average positron lifetime $\bar{\tau}$ as a function of the sample temperature in post-quench annealed Al–7.5 at.% Li–1.1 at.% Cu and in Al–7.35 at.%

Li–5.2 at.% Mg can be seen in figure 1. In figures 2 and 3 the parameters of the lifetime spectrum decomposition I_2, τ_2 and τ_1 are shown together with $\bar{\tau}$. In the temperature range between room temperature and 150 °C the $\bar{\tau}$ values in Al–Li–Cu correspond nearly completely to those found for the binary Al–Li alloy. Above 150 °C a pronounced increase in $\bar{\tau}$ is observed, which is associated with the appearance of a second lifetime component having a lifetime value of $\tau_2 - 255 \pm 5$ ps.

The precipitation sequences in Al–Li–Cu alloys [33] (see also [2–4]) have been suggested to be as follows:

$$\text{SSS} \rightarrow \text{GP zones} \rightarrow \theta'' \rightarrow \theta' \rightarrow \theta(\text{Al}_2\text{Cu})$$

$$\text{SSS} \rightarrow \text{T}_1(\text{Al}_2\text{CuLi})$$

$$\text{SSS} \rightarrow \delta' \rightarrow \delta(\text{AlLi}).$$

The relative size and volume fraction of various precipitates are functions of both composition and ageing temperature. In the binary Al–1.8 at.% Cu alloy a strong positron lifetime component appears after quenching. This component was attributed to positron trapping by vacancies associated with Cu clusters or Cu-rich GP zones [8, 34]. Other than in Al–1.8 at.% Cu in the Al–Li–Cu alloy under investigation no effect of Cu on positron lifetime and no vacancy-type lifetime component can be observed. These results correlate with transmission electron microscope (TEM) investigations by Tosten *et al* [35] and differential scanning calometric analysis by Rioja and Ludwiczak [36]. These authors observed only δ' precipitates and possibly the precursor phase to δ' in alloys of similar composition. In alloys with a higher Cu/Li concentration ratio GP(Cu) zones may be formed [37].

From TEM investigations of an Al–2.6 wt% Li–2.9 wt% Cu–0.12 wt% Zr alloy aged at 160 °C Tosten *et al* [35] found particles of the δ', θ' and T_1 phases. $\theta'(\text{Al}_2\text{Cu})$ and $\text{T}_1(\text{Al}_2\text{CuLi})$ form semicoherent platelets parallel to {0 0 1} and {1 1 1} planes, respectively. With increasing ageing time the volume fraction of T_1 and θ' increases. After 18 h ageing at 160 °C the average diameter of T_1 was 140 nm whereas the average θ' diameter was 120 nm. Overageing the alloy results in the T_1 precipitate becoming the dominant matrix phase. In addition to θ' and T_1 small fractions of $\delta(\text{AlLi})$ and $T_2(\text{Al}_6\text{CuLi}_3)$ may be formed mainly at grain boundaries.

From this discussion we may conclude that the appearance of the trapped positron lifetime component in Al–Li–Cu above 150 °C is mainly due to the formation of particles of the semicoherent $\text{T}_1(\text{Al}_2\text{CuLi})$ phase and to a smaller extent of the $\theta'(\text{Al}_2\text{Cu})$ phase. Positrons become localized at misfit dislocations of semicoherent particles resulting in a trapped positron lifetime of $\tau_2 = 255 \pm 5$ ps. The increase in the intensity of the trapped positron lifetime component I_2 (and also of $\bar{\tau}$) above 150 °C is due to the formation and growth of the particles. Coarsening of particles results in a decrease in I_2 and $\bar{\tau}$ above 250 °C. Further, above 250 °C an increasing fraction of trapped positrons annihilates at thermal vacancies. In the binary Al–1.8 at.% Cu alloy positron trapping by semicoherent θ' particles was observed above 150 °C by Dlubek [8]. The trapped positron lifetime was estimated to be $\tau_2 = 195 \pm 5$ ps. This is distinctly less than the τ_2 value in the Al–Li–Cu alloy. We may therefore conclude that in the Al–Li–Cu alloy under investigation, positron trapping by T_1 particles dominates and the trapped positron lifetime of 255 ± 5 ps is characteristic of the T_1 phase.

The precipitation sequence in the Al–Li–Mg under investigation can be described as follows [2–4, 26]:

$$\text{sss} \rightarrow \delta' \rightarrow Al_2MgLi.$$

In addition to the cubic equilibrium phase Al_2MgLi, which forms incoherent plates on {0 0 1} matrix planes, some fraction of $(Mg,Li)_{17}Al_{12}$ may also appear [38]. FIM/atom probe studies of Al–Li–Mg have indicated the presence of Mg in the δ' precipitates. At δ' composition of 17.5 ± 0.5 at.% Li and 4.9 ± 0.3 at.% Mg was estimated by Menand *et al* [39]. The estimated effect of Mg on the positron lifetime in δ' particles is only in the order of 1 ps and therefore too small to be detected.

The lifetime $\bar{\tau}$ in Al–Li–Mg is slightly greater than in Al–Li and Al–Li–Cu in the temperature range between room temperature and 130 °C (figure 1). This effect may be attributed to a small fraction of positrons trapped by quenched-in vacancy–Mg atom complexes. As observed earlier in Al–3 at.% Mg [40] quenched-in vacancy–Mg atom complexes anneal out around 100 °C.

The increase in $\bar{\tau}$ and the appearance of a distinct second lifetime component of $\tau_2 = 235 \pm 5$ ps above 200 °C may be attributed to positrons trapped at the incoherent particle–matrix interface of the Al_2MgLi phase. Formation, growth and coarsening of the Al_2MgLi particles are reflected by the behaviour of I_2 and $\bar{\tau}$. The lower average lifetimes in Al–Li–Mg compared with Al–Li–Cu are due to both lower τ_2 and lower I_2 values. The lower I_2 in Al–Li–Mg reflects the smaller volume fraction of Al_2MgLi compared with Al_2CuLi. This may be attributed to the higher solubility of Mg in the Al matrix compared to Cu. The difference between the τ_2 values of Al_2CuLi and Al_2MgLi is not easy to explain because τ_2 depends on the open volume and chemical surroundings of the site of positron localization and therefore on the microstructure of the particle–matrix interfaces of both types of precipitates. Trapped positron lifetime values from 195 to 260 ps are typical of precipitates in aluminium alloys having semicoherent or incoherent interfaces [8, 9].

4.3. Al–Li–Sc alloy

The behaviour of the average positron lifetime $\bar{\tau}$ and of the parameters τ_1, τ_2 and I_2 of lifetime spectra decomposition during post-quench annealing of Al–7.35 at.% Li–0.18 at.% Sc is shown in figures 4 and 5, respectively. In as-quenched Al–Li–Sc $\bar{\tau}$ is larger by 15 ps than in the binary Al–Li. The lifetime spectra, however, are well described by single exponentials. During annealing $\bar{\tau}$ decreases and reaches a minimum at 150 °C. Thereafter, an increase follows and a shoulder appears at about 230 °C. The increase is associated with the appearance of a second lifetime component of $\tau_2 = 245 \pm 5$ ps.

The decomposition of binary Al–Sc has been investigated by Drits *et al* [41] and Beresina *et al* [42]. Al_3Sc particles are precipitated from a supersaturated solid solution of Al–Sc. Analogous to Al_3Li and Al_3Zr, the Al_3Sc phase has a cubic $L1_2$ structure and precipitates as coherent spherical particles. Coherence is lost when the particle diameter exceeds 80 nm. Analogous to Zr [43] the addition of Sc to Al–Li has a marked effect on the δ' distribution. In the as-quenched state of the Al–Li–Sc alloy primary Al_3Sc particles were observed by Beresina *et al* [5]. The particles are nearly unaffected by solution annealing at 500 °C. Ageing of quenched Al–Li–Sc samples below the δ' solvus leads to the development of composite $\delta'(Al_3Li)/Al_3Sc$ precipitates in addition to δ'. The development of composite (or duplex) precipitates

may be described as epitactic growth of Al_3Li on Al_3Sc (like for Al_3Li/Al_3Zr [43]). In figure 6 TEM dark-field images show the microstructure of both Al–7.35 at.% Li and Al–7.35 at.% Li–0.18 at.% Sc aged for 135 h at 170 °C. The composite δ'/Al_3Sc particles that we observed also after annealing at 300 °C for 2.5 h have a larger size and greater stability than Al_3Sc-free δ' particles.

The higher positron lifetime in as-quenched Al–Li–Sc compared with Al–Li we attribute to positron trapping by primary Al_3Sc particles and by quenched-in vacancy–scandium atom complexes. These complexes anneal out below 150 °C. We observed an analogous behaviour by τ measurements in Al–0.18 at.% Sc. Around 150 °C primary Al_3Sc particles and possibly more stable Sc–vacancy agglomerates compete in positron trapping with δ' particles, resulting in the slightly higher $\bar{\tau}$ values in Al–Li–Sc compared with the Al–Li in which only the δ' phase precipitates. In Al–0.18 at.% Sc we found positron trapping by coherent Al_3Sc particles resulting in a vacancy-type second lifetime component ($\tau_2 \simeq 240$ ps). We have attributed this lifetime component to positrons localized at structural vacancies of the Al_3Sc phase. The increase in $\bar{\tau}$ in Al–Li–Sc above 170 °C (figure 4) may be attributed to an increase in the fraction of positrons trapped by composite δ'/Al_3Sc particles, which grow at the expense of Al_3Sc-free δ' particles. Positrons are captured at first by the Al_3Li shell, but they become localized finally at defects of the Al_3Li/Al_3Sc interface or at structural vacancies of the Al_3Sc core. Both types of annihilation sites would explain the vacancy-type lifetime component, the appearance of which is associated with the increase in $\bar{\tau}$ (figure 5). An increased formation of the incoherent δ(AlLi) phase due to Sc addition, which was observed in x-ray diffraction experiments [6], may also have some effect on $\bar{\tau}$. Above 300 °C positron trapping by thermal vacancies dominates the increase of $\bar{\tau}$ and of I_2.

5. Conclusions

The results of our study show that the positron annihilation technique may be used to investigate precipitation phenomena in Al–Li based alloys. A positron lifetime of 185 ± 5 ps that was observed in Al–Li is attributed to positrons annihilating from internal regions of coherent $\delta'(Al_3Li)$ phase. The δ' particles are not associated with vacancies. A very weak sensitivity of the positron lifetime to decomposition process going on in Al–Li between room temperature and 200 °C was observed. This is attributed to a preferential annihilation of positrons near ordered regions, which are rapidly formed during quenching as a precursor phase to δ'. The ordered regions may be enriched in lithium, resulting in a positron lifetime like that of δ'. The method shows a strong response to formation of semicoherent and incoherent phases such as $T_1(Al_2LiCu)$ and Al_2LiMg in Al–Li–Cu and Al–Li–Mg, respectively. Al–Li–Sc shows a special behaviour. This is attributed to positron trapping by composite $\delta'(Al_3Li)/Al_3Sc$ particles, which seem to be associated with vacancies in the δ'/Al_3Sc interface or with structural vacancies in the Al_3Sc core. We found indications of quenched-in vacancies bound to solution atoms in Al–Li–Sc and, to a smaller extent, in Al–Li–Mg but not in Al–Li–Cu and Al–Li.

Acknowledgments

We thank R Krause from Martin-Luther-University Halle for his assistance during

lifetime measurements. K Welpmann and M Peters from Institut für Werkstoff-Forschung, DLR Köln, are acknowledged for helpful discussions.

References

[1] Williams D B 1989 *Aluminium–Lithium Alloys V: Proc. 5th Int. Conf. (Williamsburg, VA, 1989)* ed T H Sanders Jr and E A Starke Jr (Birmingham: Materials and Component Engineering) p 551
[2] Sanders T H Jr and Starke E A Jr 1989 *Aluminium–Lithium Alloys V: Proc. 5th Int. Conf (Williamsburg, VA, 1989)* ed T H Sanders Jr and E A Starke Jr (Birmingham: Materials and Component Engineering) p 1
[3] Williams D B and Howell P R 1989 *Treatise on Materials Science and Technology* vol 31 (New York: Academic) p 365
[4] Quist W E and Narayanan G H 1989 *Treatise on Materials Science and Technology* vol 31 (New York: Academic) p 219
[5] Beresina A L, Volkov V A, Domashnikov B P, Trofimova L N and Chuistov K V 1986 *Metallofizika* **8(3)** 116
[6] Beresina A L, Volkov V A, Kolobnev N J and Chuistov K V 1988 *Metallofizika* **10(4)** 127
[7] Gauster W B and Wampler W R 1980 *Phil. Mag.* A **41** 145
[8] Dlubek G 1987 *Age-Hardenable Aluminium Alloys: Proc. 4th Int. Conf. (Balatonfüred, Hungary, 1986)* ed J Kovacs and J Lendvai; *Mater. Sci. Forum* **13/14** 11
[9] Dlubek G, Brümmer O and Krause R 1985 *Positron Annihilation: Proc. 7th Int. Conf. (New Delhi, India, 1985)* ed P C Jain, R M Singru and K P Gopinathan (Singapore: World Scientific) p 883
[10] Bharathi A and Chakraborty B 1988 *J. Phys. F: Met. Phys.* **18** 363
[11] Leighly H P Jr, Coleman P G and West R N 1989 *Aluminium–Lithium Alloys V: Proc. 5th Int. Conf. (Williamsburg, VA, 1989)* ed T H Sanders Jr and E A Starke Jr (Birmingham: Materials and Component Engineering) p 325
[12] del Rio J, de Diego N and Fink D 1989 *J. Phys.: Condens. Matter* **1** 4441
[13] Stott M J and Kubica P 1975 *Phys. Rev.* B **11** 1
[14] Puska M J, Lanki P and Nieminen R M 1989 *J. Phys.: Condens. Matter* **1** 6081
[15] Seeger A 1974 *Appl. Phys.* **4** 183
[16] West R N 1979 *Positrons in Solids (Topics in Current Physics 12)* ed P Hautojärvi (Berlin: Springer) p 89
[17] Nieminen R M and Manninen M J 1979 *Positrons in Solids (Topics in Current Physics 12)* ed P Hautojärvi (Berlin: Springer) p 145
[18] Dlubek G, Kabisch O and Brümmer O 1979 *Phys. Status Solidi* a **55** 509
[19] Dlubek G, Brümmer O, Yli-Kauppila J and Hautojärvi P 1981 *J. Phys. F: Met. Phys.* **11** 2525
[20] Krause R, Dlubek G, Wendrock G and Brümmer O 1986 *Scr. Metall.* **20** 1761
[21] Puska M J and Manninen M 1987 *J. Phys. F: Met. Phys.* **17** 2235
[22] Plazaola F and Puska M 1991 private communication
[23] Dlubek G and Gerber W 1991 *Phys. Status Solidi* b **163** 83
[24] Seeger A and Banhart F 1987 *Phys. Status Solidi* a **102** 171
[25] Mills A P and Wilson J R 1982 *Phys. Rev.* A **26** 490
[26] Fridlyander I N, Ambartsumyan S M, Shiryaeva N V and Gabidullin R M 1968 *Met. Sci. Head Treat. (USSR)* **3** 211
[27] Hautojärvi P and Vehanen A 1979 *Positrons in Solids (Topics in Current Physics 12)* ed P Hautojärvi (Berlin: Springer) p 1
[28] Schaefer H E, Gugelmeier R, Schmolz M and Seeger A 1985 *Microstructural Characterization of Materials by Non-Microscopical Techniques: Proc. 5th Int. Symp. on Metallurgy and Materials Science (1984)* ed N Andersen, M Eldrup, N Hansen, D J Jensen, T Leffers, H Lilkolt, O B Petersen and B N Singh (Roskilde, Denmark: Riso National Laboratory) p 489
[29] Ceresara S, Giarda H and Sanchez A 1977 *Phil. Mag.* **35** 97
[30] Khachaturyan A G, Lindsey T F and Morris J W Jr 1988 *Metall. Trans.* A **19** 249
[31] Radmilovic V, Fox A G and Thomas G 1989 *Acta Metall.* **37** 2385
[32] Al-Kassab T, Menand A, Anger P and Haasen P 1989 *J. Physique Coll.* **50** C8 419
[33] Hardy H R and Silock J M 1955–6 *J. Inst. Met.* **84** 423
[34] Gläser U H, Dlubek G and Krause R 1991 *Phys. Status Solidi* b **163** 337

[35] Tosten M H, Vasuderan A K and Howell P R 1986 *Aluminium–Lithium Alloys III: Proc. Third Int. Aluminium–Lithium Conf. (Oxford, 1986)* ed C Baker, P J Gregson, S J Harris and C J Peel (London: Institute of Metals) p 483
[36] Rioja R J and Ludwiczak E A 1986 *Aluminium–Lithium Alloys III: Proc. Third Int. Aluminium–Lithium Conf. (Oxford, 1986)* ed C Baker, P J Gregson, S J Harris and C J Peel (London: Institute of Metals) p 471
[37] Noble B, McLaughlin J R and Thompson G 1970 *Acta Metall.* **18** 339
[38] Kanani N, Abein S P and Abbaschian G R 1985 *Aluminium* **61** 5–358
[39] Menand A, Al-Kassab T, Chambreland S and Sarran J M 1988 *J. Physique Coll.* **49** C6 353
[40] Dlubek G, Brümmer O and Möser B 1981 *Phys. Status Solidi* a **63** K115
[41] Drits M E, Kadauer E S, Dobatkina T W and Turkina N J 1973 *Izv. Akad. Nauk USSR Metally* **4** 213
[42] Beresina A L, Volkov V A, Domashnikov B P and Chuistov K V 1987 *Metallofizika* **9**(5) 43
[43] Makin P L and Ralph B 1984 *J. Mater. Sci.* **19** 3835
[44] Petersen K 1983 *Positron Solid State Physics: Proc. Int. School of Physics Enrico Fermi (Varenna, 1981)* ed W Brandt and A Dupasquier (Amsterdam: North-Holland) p 298
[45] Kubica P, McKee B T A, Stewart A T and Stott M J 1975 *Phys. Rev.* B **11** 11
[46] Schaefer H E, Gluck W, Banhart F and Bauer W 1987 *Vacancies and Interstitials in Metals and Alloys* ed C Abromeit and H Wollenberger (Aldermannsdorf: Trans. Tech.) p 111
[47] Myllylä R, Karras M and Miettinen T 1977 *Appl. Phys.* **13** 387
[48] Hautojärvi P, Johansson J, Vehanen A, Yli-Kauppila J, Hillaired J and Tsanetakis P 1982 *Appl. Phys.* A **27** 49
[49] Rodda J L and Stewart M G 1963 *Phys. Rev.* **131** 255